Separation Science and Technology
Publication details, including instructions for authors and subscription information:
http://www.informaworld.com/smpp/title~content=t713708471

Modeling the Transient Adsorption Process of Ternary Mixtures on Nanoporous Zeolitic Adsorbents in Batch Systems

A. M. Avila[a]
[a] Instituto de Investigaciones en Catálisis y Petroquímica, INCAPE (FIQ, UNL - CONICET), Santa Fe, Argentina

To cite this Article Avila, A. M.(2008) 'Modeling the Transient Adsorption Process of Ternary Mixtures on Nanoporous Zeolitic Adsorbents in Batch Systems', Separation Science and Technology, 43: 4, 862 — 885
To link to this Article: DOI: 10.1080/01496390701870648
URL: http://dx.doi.org/10.1080/01496390701870648

Separation Science and Technology, 43: 862–885, 2008

ISSN 0149-6395 print/1520-5754 online
DOI: 10.1080/01496390701870648

Modeling the Transient Adsorption Process of Ternary Mixtures on Nanoporous Zeolitic Adsorbents in Batch Systems

A. M. Avila

Instituto de Investigaciones en Catálisis y Petroquímica, INCAPE (FIQ, UNL – CONICET), Santa Fe Argentina

Abstract: Transient adsorption process of a hypothetical ternary mixture constituted by a fast diffusing-weak adsorbing (C1), a low diffusing-strong adsorbing (C2), and a high saturation capacity species (C3) on zeolite adsorbents in a batch system was modeled by the Maxwell-Stefan formulation in combination with the IAST mixture isotherm. When the Henry constant of C2 and C3 were $K_2 = K_3$, the transient adsorption selectivity ($S_{i,j}$) defined with the weakest-adsorbing species used as a reference becomes higher for C3 in comparison with C2, during the entire lapse of contact time. The influence of the gas phase pressure and mixture composition on the transient adsorption selectivities basically depends on the behavior of the equilibrium selectivities ($S_{i,j}^{eq}$). The transient response of the fractional coverage (θ_i) of C1 within the zeolite overshoots its equilibrium value. In comparison to the single adsorption profiles, the component with the highest saturation capacity (C3) is the only species of the ternary mixture that maintains its fractional coverage practically unmodified. When $K_2 > K_3$, a cross-over between the corresponding equilibrium selectivities can occur with pressure. The use of the model based on experimental data is discussed.

Keywords: Multi-component systems, adsorption, diffusion, zeolites

INTRODUCTION

There has been a phenomenal growth in the development of adsorptive technologies for the separation and purification of multi-component gas

Received 31 May 2007, Accepted 4 November 2007
Address correspondence to A. M. Avila, Instituto de Investigaciones en Catálisis y Petroquímica, INCAPE (FIQ, UNL – CONICET), Santiago del Estero 2654, (S3000AOJ) Santa Fe, Argentina. E-mail: aavila@fiqus.unl.edu.ar

mixtures during the past three decades. They are being used in chemical (O_2 and N_2 from air), petrochemical (normal isoparaffin separation), environmental (CO_2 and CH_4 from landfill gas), pharmaceutical (solvent vapor recovery), and electronic gas (high-pure N_2 and H_2) industries (1). Many of the current and future challenges in the research of adsorption phenomena are orientated to miniaturized devices for microreactors and microseparators (2–4), gas sensors (5) and Lab on a Chip technologies (6). In all these areas, zeolite adsorbents have promising prospects (7).

Essentially, all catalytic and separation processes based on zeolitic materials are related to the behavior of multi-component systems. According to the diversity of new materials, there is a growing need for studying the transport properties of mixtures inside microporous solids. The interest in understanding multi-component fluid–solid contact focuses on either the experimental information obtained in the lab or the search for adequate models that could be used for macroscopic engineering calculations (8, 9). Despite its importance, however, the transport of mixtures through zeolitic solids has only recently received more thorough attention, and the latter may be due to the difficulties normally encountered in the experimentation with mixtures, as well as to the exponential increase of the simulation complexity when incorporating a large number of components (10).

Nowadays, there is a growing interest in obtaining parameter predictions of diffusion and adsorption by means of molecular simulation. The predictions capability of the new molecular models have shown a reasonable degree of accuracy and reliability (11, 12). The upcoming nanoscopic parameters become a continual source of data required for the macroscopic description of transport processes in novel zeolite material.

The mass transport of different molecules within zeolites is significantly influenced by their adsorption and diffusion characteristics and also by other parameters such as: the pore diameters, the structure of the pore walls, the interactions between the surface atoms and the diffusing molecules, the configuration of the diffusing molecules, the way the channels are interconnected, and particularly, on adsorbate–adsorbate interactions (13). With such a complex scenario, multi-component mass transfer in catalytic and separation processes is often treated considering transport models assuming homogeneous structures usually associated with diluted solutions. Although experimental data are available on adsorption of pure hydrocarbons for various zeolites, they are scarce for mixture sorption phenomena considering the increasing demand associated with the potential separation processes.

It is generally accepted that the generalized Maxwell–Stefan formulation offers the most convenient and the nearest quantitative prediction of multi-component diffusion through zeolite crystals (14). The strength of this model lies in the fact that it intrinsically encompasses intra-crystalline diffusion phenomena as well as adsorption processes, facilitating the prediction of multi-component diffusion, based on pure component Maxwell–Stefan diffusivities and mixture adsorption isotherms. Also, the Ideal

Adsorbed Solution Theory (IAST) (15) proved to be an adequate model for representing adsorption of mixtures of species with different saturation capacities (16). Thus, by using diffusion and adsorption parameters defined for single species on a given zeolitic material provided by nanoscopic models and a macroscopic model such as the Maxwell-Stefan equations mentioned above, it would be possible to obtain predictions of the transient adsorption of mixtures. Consequently, for design and engineering calculations, there is a growing need for a systematic knowledge and handling of the simulation of adsorption processes of mixtures based on macroscopic models including nanoscopic parameters. By achieving this, a fast screening computational approach will be provided to evaluate the performance of different zeolite adsorbents for potential separation processes. Moreover, the ability to predict the transient behavior of multi-component gas mixtures becomes very useful for analysing the dynamic response of microreactors, gas sensing, or any other Lab on a Chip devices. In this sense, transient response profiles can provide additional valuable information because adsorption and diffusion phenomena can be distinguished, and therefore analysed separately.

Most of the works reported on transient adsorption response of mixtures in zeolite adsorbents consider binary systems and extended Langmuir isotherm (17, 18). However, works on dynamic adsorption of ternary mixtures are rather scarce (19) and even rarer which are about transient adsorption with the mixture isotherm described by the IAST model (20).

This work examines the modeling and simulation results for transient adsorption processes of ternary mixtures on zeolitic adsorbents in batch systems. The objective is to determine the type of behavior expected in transient experiments by analysing the following criteria:

a. Adsorption selectivity values and the effect of operation variables such as contact time, pressure and gas phase composition.
b. Transient profiles of fractional coverages and their comparison with those of single components.

The dynamics simulation does not deal with experimental data, it focuses on predicting the mixture behavior for certain assumed parameter combinations. An example of using the model for the treatment of the experimental data in the evaluation of a zeolite-based catalyst is shown in the last section.

MODELING THE BATCH ADSORPTION PROCESS

In this work, a batch adsorber with a high gas recirculation rate, achieving a well-mixed device is considered (Fig. 1a). Such characteristics ensure a high value of the Biot number, which allows to neglect any mass transport resistance at the external side of the adsorbent particles in relation to

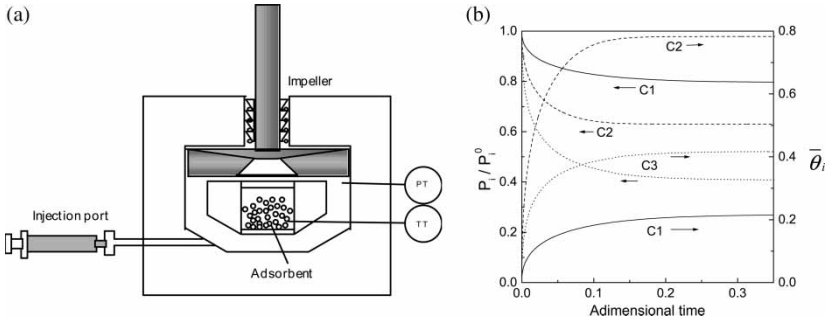

Figure 1. (a) Sketch of the proposed batch adsorber. (b) Transient responses of the partial pressure (P_i) and fractional coverage ($\bar{\theta}_i$) for single components C1 (solid line), C2 (dashed lined) and C3 (dotted line) to a pulse increase ($P_i = 0,\ t < 0$; $P_i^0 = 23$ kPa, $t = 0$) in the gas phase mass. Adimensional time: $D_{0,i}\ (t/r_c^2)$.

internal restrictions (21). The unit operates isothermally at constant volume of the gas mixture. The gas phase obeys the ideal gas law equation.

The Zeolite Particle

Zeolites are materials with very constrained structures so that often no distinction between diffusing and adsorbed species can be made. Since the diffusing molecules never escape from the force field of the pore walls, the fluid within the pore can be considered as a single "adsorbed" phase (22). Diffusion within this regime is called in different ways, e.g., configurational diffusion, intracrystalline diffusion, micropore diffusion, or simply surface diffusion, (23). According to this approach the mass balances for the various hydrocarbons inside the zeolite crystals can be written as:

$$\rho_z \frac{\partial q_i(r,t)}{\partial t} = -\frac{1}{r^2}\frac{\partial}{\partial r}\left(r^2 N_i\right) \tag{1}$$

where q_i is the adsorbate concentration, N_i is the molar flux of each species, and ρ_z is the zeolite density. An adequate model of the configurational diffusion flux is the generalized Maxwell – Stefan model (14). The fluxes of each species in the mixture can be described by

$$\underline{N} = -\rho_z \, \mathrm{q}_s \, \mathrm{B}^{-1} \, \Gamma \underline{\nabla} \theta \tag{2}$$

where

$$\Gamma_{ij} \equiv \frac{\theta_i}{P_i}\frac{\partial P_i}{\partial \theta_j} \qquad B_{ii} = \sum_{j=1/j\neq i}^{n} \frac{\theta_j}{D_{0,ij}} + \frac{1}{D_{0,i}} \qquad B_{ij} = -\frac{\theta_i}{D_{0,ij}}; \quad i \neq j \tag{3}$$

$$q_{s,ii} = q_{s,i} \qquad q_{s,ij} = 0; \quad i \neq j \tag{4}$$

and $\underline{N}$ and $\underline{\nabla}\theta$ are the multi-component vectors of flow and fractional coverage gradient, respectively. $D_{0,ij}$ can be estimated according to the Vignes equation (24)

$$D_{0,ij} = \left(D_{0,i}\right)^{\frac{\theta_i}{\theta_i+\theta_j}}\left(D_{0,j}\right)^{\frac{\theta_j}{\theta_i+\theta_j}} \tag{5}$$

The thermodynamic correction factor Γ (Eq. (2)) is a matrix that depends on the mixture isotherm characteristics. The mixture fractional coverages are estimated from pure component isotherms using the IAST model. Basically, the equation of IAST theory is the analogue of Raoult's law for vapor-liquid equilibrium, i.e.

$$Py_i = x_i P_i^*(\pi) \qquad i = 1, 2, \ldots, n \tag{6}$$

where x_i is the mole fraction in the adsorbed phase

$$x_i = \frac{\theta_i}{\sum_i^n \theta_i} \tag{7}$$

and $P_i^*(\pi)$ is the pressure for sorption of every pure component i, which yields the same spreading pressure, π, as that for the mixture. The spreading pressure is defined by the Gibbs adsorption isotherm (25)

$$\frac{\pi A}{RT} = \int_0^{P_i^*} \frac{q_{i,s}\theta_{i,pure}^{eq}(P)}{P} dP \tag{8}$$

where A is the adsorbent area and $\theta_{i,pure}^{eq}(P)$ is the pure component isotherm.

However, for this model, the partial derivatives needed for calculating Γ_{ij} cannot be expressed explicitly, thus a numerical resolution is required.

Note that the assumption that the process takes place under isothermal condition is only valid when diffusion time of mass transfer is longer than the characteristic time delay for heat transfer. Otherwise, a thermal driving force should be taken into account in addition to a chemical driving force, because thermal conduction may become comparable or the rate-limiting step in the description of adsorption-diffusion process in nanoporous materials. Some criterion for considering negligible heat effects can be found in Brandani et al. (26) and Silva et al. (27).

THE GAS PHASE

The integral mass balance in the gas phase can be expressed as:

$$\frac{V_{gp}}{RT}\frac{dP_i}{dt} = -\int_{V_{gp}} \underline{\nabla} \cdot \underline{N}_i dV \tag{9}$$

which, coupled to the integral mass balance in the solid particles,

$$m_z \frac{d\,\bar{q}_i}{dt} = -\int_{V_z} \underline{\nabla} \cdot \underline{N}_i dV \tag{10}$$

results in:

$$\frac{V_{gp}}{RT}\frac{dP_i}{dt} = -m_z \frac{d\bar{q}_i}{dt} \tag{11}$$

where the volume – averaged adsorbate concentration can be defined as

$$\bar{q}_i = \frac{3}{r_c^3}\int_0^{r_c} q_i r^2 dr \tag{12}$$

Equations (1) and (11) are subjected to the following initial and boundary conditions

$$t = 0 \qquad 0 \le r \le r_c \qquad q_i(r,0) = 0 \qquad P_i = P_i^0 \tag{13}$$

$$r = 0 \qquad \frac{\partial q_i}{\partial r}(0,t) = 0 \tag{14}$$

$$r = r_c \qquad q_i(r_c,t) = IAST(P, y_i) \tag{15}$$

Solution of the Proposed Model

The numerical solution of the partial differential equations of the model proposed for the diffusion–adsorption process was achieved using the method of lines (MOL), that converts partial differential equations into a system of ordinary differential equations (28). The approach used in the ternary adsorption evaluation was based on Krishna and Baur 2003 (29). The numerical calculations were done with Matlab 6.5. The zeolite particle radius r_c was assumed to be 0.5 μm. The adsorbent mass m_z, the gas phase volume and the temperature of the batch system relate to each other as $(m_z RT)/(V_{gp}) = 21.7$ (kPa Kg mol^{-1}). The rest of the zeolite parameters used in the model are shown in Table 1.

RESULTS AND DISCUSSION

A ternary mixture with different individual adsorption and diffusion properties was considered. As shown in Table 1 the component 1 (C1) is a fast diffusing–weak adsorbing species, the component 2 (C2) stands for a low diffusing–strong adsorbing molecule and a high saturation capacity

Table 1. Parameters of adsorption and diffusion in the zeolite

Component	C1	C2	C3
$q_{i,s}$ (mol Kg $^{-1}$)	1	0.5	1.5
b_i (kPa^{-1}) $\times 10^2$	1.45	21.75	7.25
$D_{0,i}$ (m^2 s $^{-1}$) $\times 10^{15}$	1.5	0.5	1

species with intermediate adsorption and diffusion characteristics is represented by component 3 (C3). Pure component isotherms responding to the Langmuir model were selected. The parameters values assigned to the model relate each other as follows: $q_{1,s} = 2q_{2,s}$, $q_{3,s} = 3q_{2,s}$; $b_2 = 15b_1$, $b_3 = 5b_1$; $D_{0,1} = 3D_{0,2}$, $D_{0,3} = 2D_{0,2}$, corresponding to the case when the Henry constants ($K_i = q_{i,s}b_i$) are $K_2 = K_3 > K_1$. The diffusion and adsorption parameters used in the model are characteristic values that can be found in the oil refining processes with zeolite-based catalysts. For instance, in the hydrocracking of n-alkane mixture on Pt/H-zeolite (30), or in the isomerization process of n-hexane with MFI zeolite (31). The particle diameter of 0.5 microns is a typical magnitude for the zeolite crystals used as catalyst or adsorbents in this kind of processes. Although the selected properties used in the model are in the same order of magnitude as those reported for hydrocarbons adsorption on Y or MFI-type zeolites, the same effects can indeed be found in other nanoporous systems with diffusing molecules sizes close to pore diameter (20).

Single Adsorption

The proposed model can be particularized for the case of adsorption process of an individual component. In this case, equation (1) can be expressed as

$$\frac{\partial \theta_i(r,t)}{\partial t} = -\frac{1}{r^2}\frac{\partial}{\partial r}\left(r^2 D_{0,i}\Gamma \frac{\partial \theta_i}{\partial r}\right) \tag{16}$$

Figure 1 shows that a pulse change in the feed mass rate entering the batch adsorber renders an instantaneous and maximum value of pressure, P_i^0, in the gas phase (initial condition of the model). Further to this point, the gas phase pressure decreases as the component gets adsorbed on the microporous solid causing the change of the uptake rate of each species. A comparison among the shapes of the uptake curves is presented in Fig. 1b. The adsorbate concentration profiles are expressed as the volume-averaged fractional coverage in the particle ($\bar{\theta}_i$) as function of adimensional time defined as $\tau = D_{0,i}\, t/r_c^2$. Figure 1b shows that the fractional approach to equilibrium is faster when increasing non-linearity–higher b_i values (see Table 1) which has already been observed in several previous experimental studies (32–34). The latter is taken into account by the model as it considers that the driving

force for diffusive transport is the gradient of chemical potential, rather than the gradient of concentration, as assumed in the Fick formulation (14, 32). In adsorption systems when the equilibrium isotherm is linear, the Fick diffusivity D_i (also known as transport diffusivity) is generally constant (independent of the concentration). However, when the isotherm is non-linear, as in this case, the diffusivity is generally concentration dependent. Moreover, in the case of a type I Langmuir isotherm, the thermodynamic correction factor becomes $\Gamma = 1/(1-\theta_i)$ which enhances the transport diffusivity $D_i = D_{0,i}\Gamma$ as the fractional coverage θ_i increases. According to this, the fastest uptake rate in terms of fractional approach to equilibrium, is for C2 in correspondence to its highest value of the Langmuir parameter b_i.

Additionally, in a batch system, the changes of gas phase concentration influence the overall transport process. The partial pressure evolution of the species in the gas phase shown in Fig. 1 reflects the difference between adsorption rates in terms of the adsorbed molar amounts according to Eq. (11). The pressure decay of C3 is more pronounced in this case, indicating a faster adsorption kinetics than the other species in terms of molar rates.

In order to make comparisons among the adsorption characteristics of the species, a selectivity or separation factor ($S_{i,j}$) should be defined and, although $S_{i,j}$ may be expressed in different ways, in this work it was considered as follows:

$$S_{i,j} = \frac{\bar{\theta}_i/P_i}{\bar{\theta}_j/P_j} \tag{17}$$

where $\bar{\theta}_i$ is the volume-averaged fractional coverage in the particle and P_i the partial pressure in the gas phase of C2 and C3. The lowest-adsorbing component C1 was designated as a reference species (index j).

The single adsorption selectivities (also called ideal selectities) for C2 and C3 in relation to C1, i.e., $S_{2,1}$ and $S_{3,1}$, are exhibited in Fig. 2. $S_{2,1}$ is higher than $S_{3,1}$ and both values increase continuously with the contact time arriving at a plateau after 60 seconds, where they take the single equilibrium values corresponding to the final pressure in the gas phase. Several authors (35, 36) have reported single or ideal selectivities as a rough estimate of the material separation capacity. However, due to this rather simplistic approach, such ideal selectivity values cannot depict the real performance of the materials under process conditions dealing with multi-component systems. The actual mixture selectivities are expected to be rather different from those estimated for individual components. Hence, as it is well established, the use of ideal selectivities for the prediction of separation performance of gas mixtures in zeolite adsorbents is not recommendable.

Mixture Adsorption

The time response of the adsorption process for a pulse increase of the mass entering to the batch system can be visualized in Fig. 3. The fractional

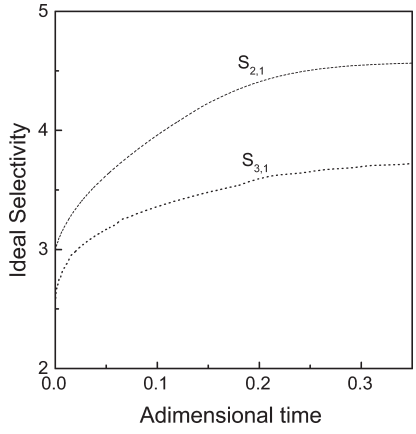

Figure 2. Ideal selectivities ($S_{i,j}$) of individual components C2 and C3 with respect to C1 versus adimensional time, $P_i^0 = 23$ kPa.

coverage is higher for C3 according to its higher saturation capacity. The transient profiles of the fractional coverages respond to the coupling effects arising in diffusion of mixtures of species in microporous solids such as zeolites. The different adsorption rates of the species in the mixture produce a variation of the molar fractions in the gas phase as a function of time. While the molar fractions y_1 and y_2 increase slightly with time, y_3 declines (Fig. 3).

The selectivity calculation as defined by Eq. (17) allows the comparison of the mixture adsorption behavior. Figure 4 shows that the selectivity of the

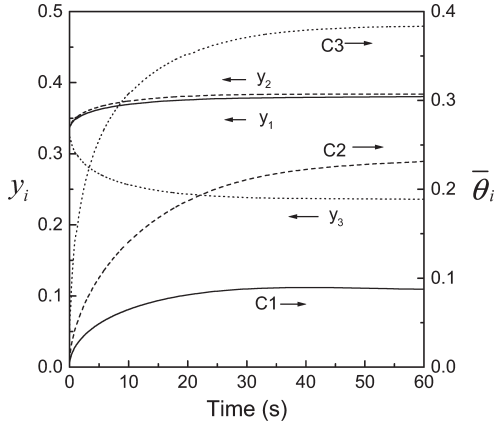

Figure 3. Transient responses of the molar fractions (y_i) and fractional coverages ($\bar{\theta}_i$) for the ternary mixture to a pulse increase in the gas phase mass. $P = 0$, $t < 0$; $P^0 =$ 69 kPa (equimolar mixture), $t = 0$.

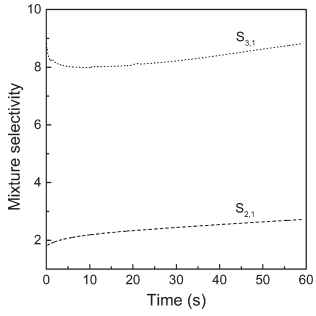

Figure 4. Mixture selectivities ($S_{i,j}$) of the components C2 and C3 with respect to C1 as function of contact time. $P^0 = 69$ kPa (equimolar mixture).

mixture components change radically not only in magnitude but also in the evolution profile, regarding the ideal selectivities of individual components calculated previously and presented in Fig. 2. The selectivity of the component with higher saturation capacity $S_{3,1}$ becomes much higher than that of the strongest adsorbing component $S_{2,1}$. Note that $S_{3,1}$ decreases slightly during the first seconds of contact time between the gas mixture and the adsorbent solid but increases further on with the contact time. The selectivity $S_{2,1}$ profile increases moderately with time and does not present slope sign changes.

The Effect of Pressure

In Figs. 5a and 5b, the transient evolution of the mixture selectivities at different pulse magnitudes of the mass fed to the batch system reveals the

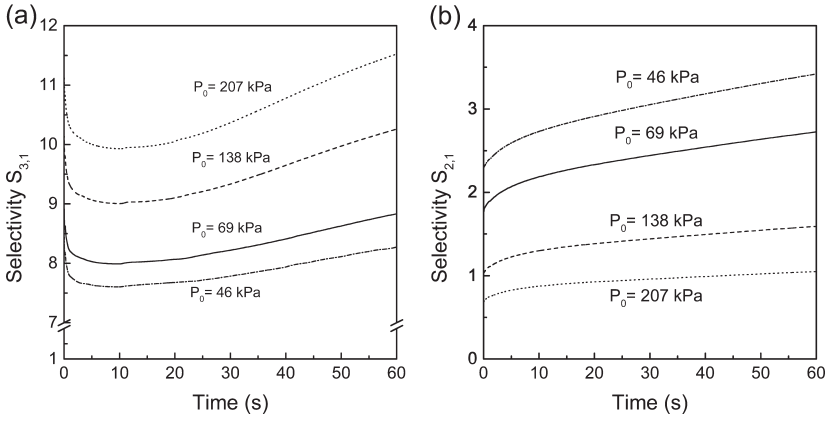

Figure 5. Mixture selectivities $S^{eq}_{3,1}$ (a) and $S^{eq}_{2,1}$ (b) as a function of contact time at different magnitudes of equimolar pulse increases.

effect of pressure on adsorption selectivities. The range of pressure used is in agreement with those values commonly found in the oil refining processes. The simulation results for an equimolar gas mixture fed to the batch adsorber show that selectivity $S_{3,1}$ increases with the gas phase pressure. On the contrary, the selectivity $S_{2,1}$ declines as the pressure grows. This particular behavior for the mixture can be understood when equilibrium selectivities estimated according to the IAST isotherm are visualized (see Fig. 6). The increase of pressure enhances the adsorption selectivity ($S_{3,1}$) for the component with the highest saturation capacity (e.g. C3), whereas the equilibrium selectivity of C2, the component with the smallest adsorption

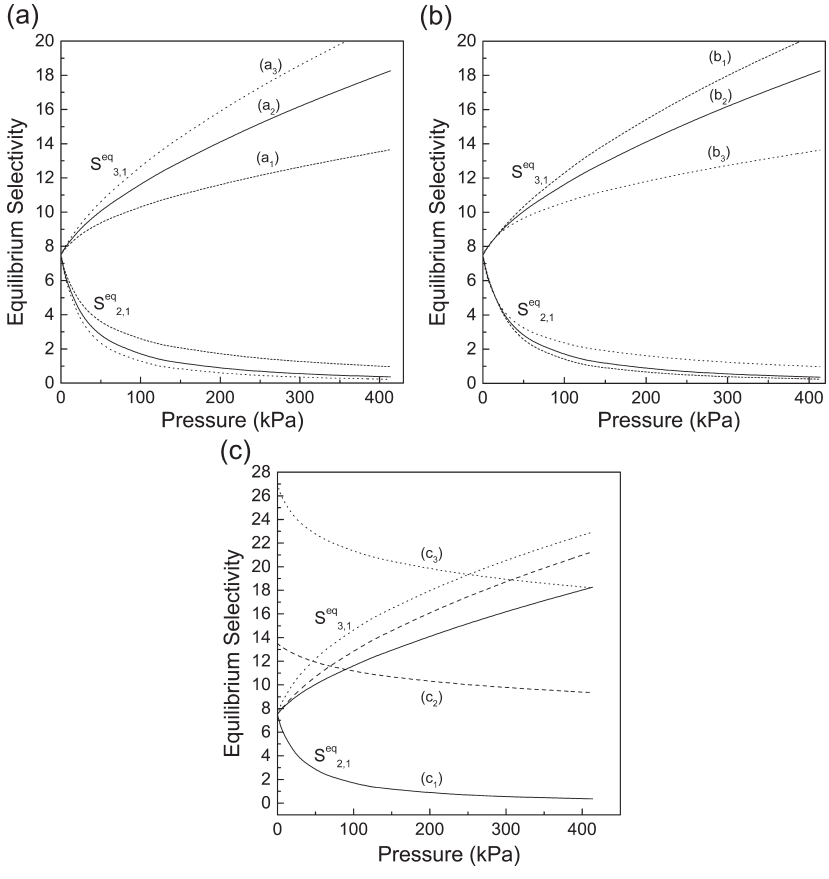

Figure 6. Equilibrium selectivities $S_{3,1}$ and $S_{2,1}$ as a function of pressure evaluated for different fraction molar according to the IAST theory. In (a) $y_{0,1}$: $y_{0,2} = 1$ and $y_{0,3}$ corresponds to 0.1 (a_1), 0.33 (a_2) and 0.5 (a_3). In (b) $y_{0,1}$:$y_{0,3} = 1$ and $y_{0,2}$ corresponds to 0.1 (b_1), 0.33 (b_2) and 0.8 (b_3). In (c) equimolar mixture and different relationships between $K_2 = q_{2,s}b_2$ and $K_3 = q_{3,s}\ b_3$, i.e., $K_2 = K_3$ (c_1), $K_2 = 1.8\ K_3$ (c_2) and $K_2 = 3.6\ K_3$(c_3).

saturation capacity ($S_{2,1}$), decreases considerably. These phenomena are known as entropic effects which are well described in the literature (37, 38). Entropy effects due to size or configuration of the molecules in a mixture adsorbing on a porous solid may appear, if the maximum amounts that can be adsorbed for the various species differ significantly. In that sense, it should be expected that higher pressures may cause smaller molecules to be packed more closely in the zeolite cages, thus increasing their adsorption and making $S_{2,1}^{eq}$ decrease and conversely $S_{3,1}^{eq}$ increase. Analogously, $S_{3,2}^{eq}$ increases with pressure according to the different values of $q_{2,s}$ and $q_{3,s}$ (Table 1). Since C2 is either a larger or bulkier molecule than C3, the latter can pack more efficiently within the zeolite channels.

At very low pressure, the equilibrium selectivities curves do approach the Henry selectivities which, in this particular case, take the same magnitude, i.e., $S_{2,1}^{eq-H} = S_{3,1}^{eq-H} = 7.5$. However, at high pressure, the equilibrium selectivity $S_{3,1}^{eq}$ is considerably larger than $S_{2,1}^{eq}$. Note that $S_{2,1}^{eq}$ takes values below 1 at pressure higher than 150 kPa. Consequently, the increase of pressure favors the adsorption of species with the highest saturation capacity. In this sense, such effect of pressure on adsorption selectivity has been useful in several separation processes investigated during the last years (39, 40). Also, the effect of pressure on the equilibrium selectivity can be the cause of a cross-over between the equilibrium selectivities $S_{2,1}^{eq}$ and $S_{3,1}^{eq}$ when $K_2 > K_3$ as shown in Fig. 6c. For instance, when $K_2 = 1.8K_3$ the cross-over pressure results at about 60 kPa and 250 kPa when $K_2 = 3.6K_3$. For instance, this effect was observed and modeled by Calero et al. (2004) (41) using Grand Canonical Monte Carlo (GCMC) techniques for the adsorption isotherm of an equimolar mixture of n-nonane and n-heptane in NaY zeolite at 230°C.

Krishna et al. (2002) (37) have studied the isotherm characteristic of various binary, ternary, and quaternary mixtures of alkanes in MFI zeolite using Configurational Bias Monte Carlo (CBMC) simulation, suggesting that entropy effects have a significant influence on mixture adsorption equilibria. They have also demonstrated that the different mixture isotherms could be accurately predicted by using IAST, showing the value of this model for engineering calculation of separation processes that may have potential commercial applications.

The Effect of Gas Composition

Different compositions of the feed gas mixture affect the adsorption equilibrium and consequently the selectivities during the transient adsorption process. Figure 7 shows the effect of a change of the concentration of the component C3 with the highest adsorption saturation capacity on the selectivities $S_{3,1}$ and $S_{2,1}$ during the first 60 seconds of contact. In all cases an equimolar ratio between the components C1 and C2 was kept. It can be noticed that the

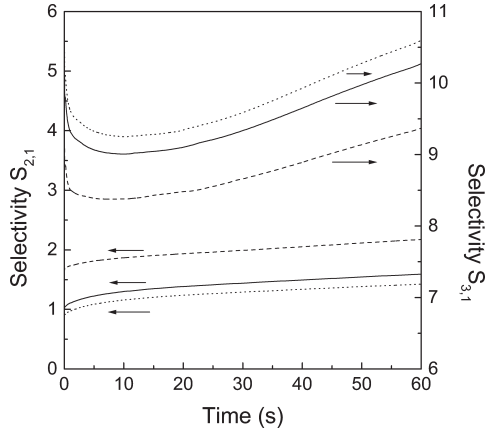

Figure 7. Transient profile of the mixture selectivities at different molar fractions $y_{0,3}$ at the time of the pulse increase. $P^0 = 138$ kPa; $y_{0,1}$: $y_{0,2} = 1$; $y_{0,3} = 0.10$ (dashed line), $y_{0,3} = 0.33$ (solid line), $y_{0,3} = 0.40$ (dotted line).

higher the molar fraction y_3 the higher the selectivity $S_{3,1}$. On the contrary, the increase of the mole fraction y_3 makes selectivity $S_{2,1}$ decrease. This effect was somehow suggested by the results presented in Fig. 6a and predicted by the IAST model. The equilibrium selectivity $S_{3,1}^{eq}$ increases with the molar fraction of component 3, while $S_{2,1}^{eq}$ behaves in the opposite way. The effect of the variation of the molar fraction of component 2, the one with the slowest diffusion and strongest adsorption can also be analyzed. The changes of the selectivities during the first 60 seconds of contact are depicted in Fig. 8 and their equilibrium counterparts are visualized in Fig. 6b. Likewise, the transient selectivities respond according to the variation of the equilibrium values. This means that an increase of the mole fraction of component 2 causes $S_{2,1}$ to increase and $S_{3,1}$ to decrease.

Experimental information about the ternary mixture equilibrium on zeolite material is rather scarce and will become worse if the demand of such data for novel adsorption separation processes increases. In contrast, several reports on this matter can be found in the literature for binary mixtures. For instance, the new potential application of H_2 purification, based on in-situ CO_2 removal in the fuel-processing unit, led to Wirawan and Creaser (2006) (19) to study the effect of the co-adsorbed species, H_2 and CO_2, on the CO_2 adsorption behavior on BaZSM-5 zeolite. They showed that the CO_2 adsorption capacity was significantly higher than that of CO on BaZSM-5. The variation of the partial pressures in the CO/CO_2 binary mixture at constant total pressure showed a systematic decrease in CO uptake with increasing CO_2 uptake. The presence of H_2 during H_2/CO_2 adsorption, increased the CO_2 adsorption capacity of BaZSM-5, due mostly to a greater quantity of strongly adsorbed species. Thus, an extended Langmuir model failed to predict the H_2/CO_2

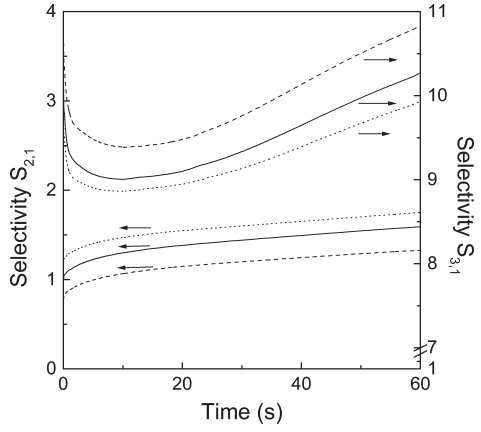

Figure 8. Transient profile of the mixture selectivities at different molar fractions $y_{0,2}$ at the time of the pulse increase. $P^0 = 138$ kPa; $y_{0,1}$: $y_{0,3} = 1$; $y_{0,2} = 0.10$ (dashed line), $y_{0,2} = 0.33$ (solid line), $y_{0,2} = 0.50$ (dotted line).

binary adsorption behavior. Peng et al. (2005) (42) determined the adsorption equilibrium of single and mixtures of propylene and ethylene. In this case, both the IAST and the extended Langmuir model predict well the binary adsorption equilibrium data under higher molar fraction of propylene in the gas phase. At low molar fraction of propylene in the gas phase, the predicted results deviate slightly from the experimental data. Schuring et al. (2001) (43) reported the loadings of both n-hexane and 2-methyl-pentane, as well as the total loading, as a function of the gas phase mixture composition. The results showed a small deviation from a linear dependence on the mixture composition ratio indicating a small preferential adsorption for n-hexane compared to its monobranched isomer. Cottier et al (1997) (44), for example, found that for the adsorption of a mixture of para- and ortho-xylene in various Y-type zeolites, both components essentially behaved similarly to the single-component case and adsorbed independently. A completely different behavior was observed for ethane and ethylene in zeolite 13X by Buffham et al. (1999) (45), where the ethylene was preferentially adsorbed at low ethane partial pressures. Thus, a nonlinear dependence was observed. Yu et al. (2006) (46) reported adsorption of benzene binary mixtures on silicalite-1 and NaX zeolites. From their experiments, they could show that the equilibrium adsorption selectivities can be severely modified according to changes of the existing mixture composition in the bulk phase.

Transient Profiles of Adsorbate Concentrations

The interplay between diffusion and adsorption processes can be understood more clearly when the adsorbate concentration profiles within the zeolite

crystal are visualized. The time responses of fractional coverages at the border ($r = r_c$), in the middle ($r = r_c/2$) and at the center ($r = 0$) of the particle can be seen in Fig. 9.

The changes of the adsorbate concentration at the border of the particle respond to the variation of molar fractions in the gas phase. Regarding the transient responses of y_i presented in Fig. 3, the fractional coverage profiles of C1 and C2 at $r = r_c$ increase with time (Fig. 9a and 9b), while that of C3 decreases (Fig. 9c). The variation of the adsorbate concentration on the border affects the transport rates of the species.

The fastest-diffusing component C1 produces an overshooting of its concentration profile (47). The curve for C1 shows a slight maximum at $r = r_c/2$ (Fig. 9b) and becomes more notorious at $r = 0$ (Fig. 9c). Such behavior is the result of the difference in transport rates among the species, particularly between C1 and C2 as can be inferred from Fig. 9c. From a physical point

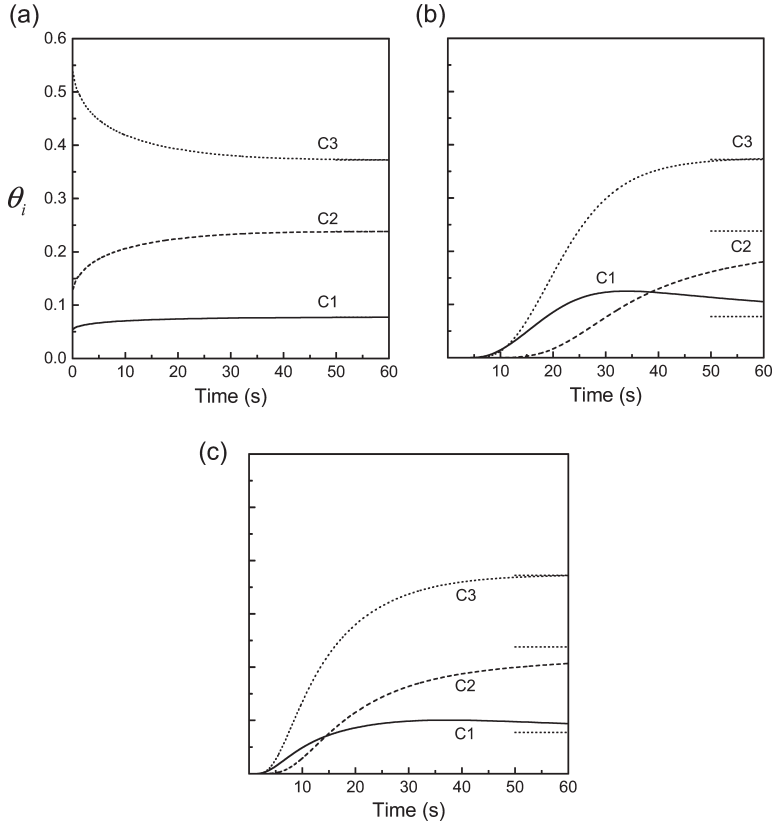

Figure 9. Transient profiles of the fractional coverages θ_i at the border $r = r_c$ (a), in the middle $r = r_c/2$ (b) and the center $r = 0$ (c) of the zeolite particle. $P^0 = 69$ kPa (equimolar mixture).

of view, this behavior can be explained as the result of the higher diffusivity of C1 that allows this species to penetrate faster into the particle, achieving a larger initial coverage; then C2, with a lower diffusivity and stronger adsorption properties, displaces C1 from the adsorption sites.

Although C3 has a lower diffusivity than C1, the latter does not penetrate faster than C3. The fractional coverage of C3 remains higher than that of C1 at any time and position inside the particle. This effect can be interpreted as the result of the interaction between diffusion and adsorption in the zeolite micropores affecting the transport rates of the species. As shown by equation (2), the characteristics of the adsorption of the mixture influence the flows of the species by setting the magnitudes of the driving forces $\nabla\theta$ and by contributing to the coupling of the diffusion processes due to the presence of the nondiagonal elements in the matrix of the thermodynamical correction factors Γ. This clearly demonstrates the importance of an adequate evaluation of the mixture isotherm, in order to provide reliable predicted values.

Similarly, the transient profiles as a function of the particle radius represent the coupling effects among the species. The fractional coverage for C1 slightly overshoots the corresponding equilibrium value at the border of the particle. The maximum concentration exhibited by C1 along the radial distance is dependent on time and its magnitude increases towards the center of the particle (Fig. 10a). Another clear distinction feature of the profiles of C1 from those of C2 and C3 (see Figures 10b and 10c) is the fact that C1 presents zones with a negative gradient for the diffusion flux, e.g., curves after $t = 15$ s in Fig. 10a.

The behavior of mixtures in transient adsorption can be compared to that of the single components at the same partial pressures. The transient profiles of the fractional coverage in the middle of the particle for each species, on the one hand, as a single component, and, on the other hand, as a constituent of the ternary mixture, are depicted in in Fig. 11. It can be observed that the fractional coverages of C1 and C2 in the mixture decrease in relation to their corresponding value for the single adsorption case. Additionally, a small maximum is observed in the C1 profile as mentioned previously. In contrast, the fractional coverages of C3 are virtually unaffected by the presence of the other species.

It should be noted that the transient mixture adsorption is determined by the combination of the heats and entropies of adsorption, and the diffusivities of the different components. Hence, depending on which effect dominates, this will determine the dynamic adsorption behavior of the mixture. In this case, the higher adsorption strength of C2 (higher value of the parameter b_2) does not compensate its lower packing entropy (lowest saturation capacity $q_{2,s}$) and diffusivity $D_{0,2}$ which brings about that C3, with the highest saturation capacity $q_{3,s}$, dominates the adsorption process due to its higher packing entropy. Consequently, C3 achieves a higher fractional coverage in the mixture (similar values as in the single component case) rendering a higher adsorption selectivity.

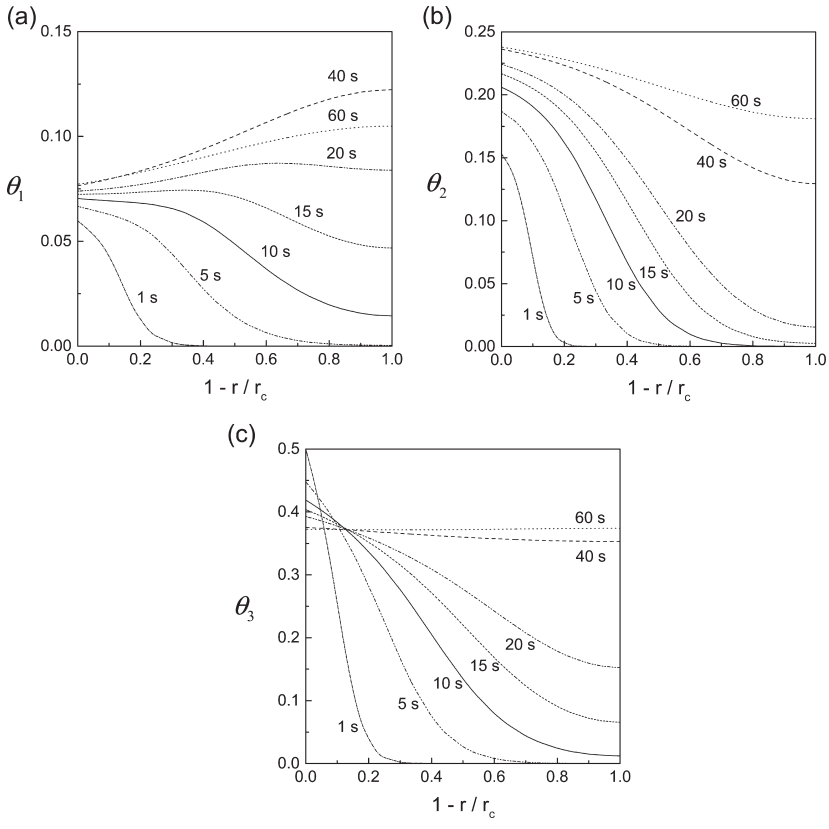

Figure 10. Fractional coverage (θ_i) profiles as a function of radial distance at different contact times of C1 (a), C2 (b), and C3 (c) in the presence of the other components. $P^0 = 69$ kPa (equimolar mixture).

It is clear that experimental information obtained from single adsorption process is not enough to explain the mixture behavior based on the interaction effects among the adsorbate molecules at high coverage in the zeolites. For this reason, experimental information on adsorption of mixtures on nanoporous adsorbents are receiving more attention lately.

Use of the Model in Catalyst Evaluation

The usefulness of the model becomes apparent through the evaluation of zeolites and zeolitic catalysts with different adsorption and diffusion characteristics. As an example, the model was used for the assessment of diffusion parameters of hydrocarbons in a cracking zeolite Y-based catalyst at 250°C, in a single-component adsorption process. By using a CREC

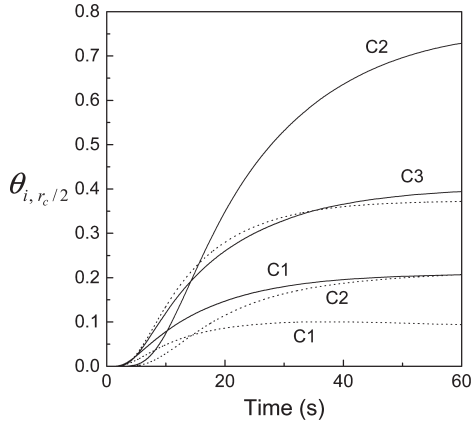

Figure 11. Fractional coverage profiles of C1, C2, and C3 estimated as single components (solid line) or taking part of the equimolar mixture (dotted line) at the middle radial distance of the particle ($r = r_c/2$). $P^0 = 23$ kPa (single), $P^0 = 69$ kPa (mixture).

Riser Simulator (48) as a batch adsorber, the intra-crystalline diffusivities of n-hexane, n-decane, and toluene were estimated using a constant volume method. More details of the experiments can be found in Avila et al. (2007a). Figure 12 shows that values predicted by the model fitted very well with experimental data of the pressure decay observed for each of the hydrocarbons. The deviations observed at initial time are due to the vaporization of the liquid hydrocarbons amounts injected to the system.

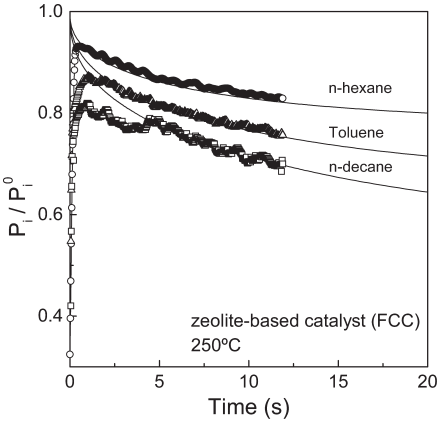

Figure 12. Pressure decay of n-hexane (○), n-decane (□), and toluene (Δ) for a pulse injection of 0.05 ml of each hydrocarbon individually in a batch adsorber (CREC Riser Simulator). Adsorbent: Y-type zeolite based catalyst (ca. 1 g). Temperature: 250°C. Solid line: simulated pressure with the proposed model. Parameters from Avila et al. (2007a).

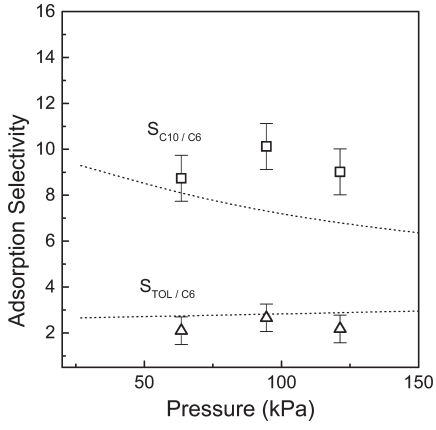

Figure 13. Comparison between simulated and experimental values of the apparent adsorption selectivities of decane and toluene in the ternary mixture with molar relationships 64.2:12.0:23.8 of n-hexane, n-decane and toluene respectively. Temperature: 250°C. Contact time: 10 s. Adsorbent: Y-type zeolite based catalyst (ca. 1 g). Feed inyected volume: 0.10; 0.15, and 0.20 ml. Parameters from Avila et al. (2007a).

The model was also used to get insight of the adsorption behavior of a ternary mixture of the same hydrocarbons, i.e., n-hexane, n-decane, and toluene. The multi-component diffusion–adsorption process in the catalyst particles was described by this model considering the zeolitic material in the compound catalyst to be the characteristic space. The apparent selectivities for different injected volumes were measured at a given contact time (10 s) between the gas mixture and the catalyst. The measurements were carried out by monitoring the gas phase pressure and analysing gas phase composition. The predictions of the apparent selectivities in the ternary mixture were close to the experimental values as shown in Fig. 13. A detailed experimental description can be found in Avila et al. (2007b) (49).

SUMMARY

The dynamics adsorption on zeolite adsorbents of a ternary mixture made up of components whose adsorption and diffusion properties present the following relationships: $q_{1,s} = 2q_{2,s}$, $q_{3,s} = 3q_{2,s}$; $b_2 = 15b_1$, $b_3 = 5b_1$; $D_{0,1} = 3D_{0,2}$, $D_{0,3} = 2D_{0,2}$, corresponding to the case when $K_2 = K_3 > K_1$.

Shows that:

i. The mixture selectivities differ significantly from the corresponding ideal values, e.g., those obtained for the adsorption processes of pure components.

ii. The adsorption selectivity of the component with the highest saturation capacity ($S_{3,1}$) becomes much higher than that of the strongest — adsorbing species ($S_{2,1}$), during the entire lapse of contact time. $S_{3,1}$ declines a little after a short contact time but recovers later, increasing slightly up to reach the equilibrium value. At different gas phase pressures, both selectivities follow the same trend as their equilibrium counterparts. While $S_{3,1}$ increases markedly with pressure, $S_{2,1}$ drops. An increase of the mole fraction of C3 enhances its selectivity, whereas the selectivity of C2, on the contrary, deteriorates. An increase of the mole fraction of C2 causes $S_{2,1}$ to rise and $S_{3,1}$ to decrease.

iii. The transient response of the fractional coverages are related to the interplay between diffusion and adsorption phenomena inside the zeolite microporous. The fastest-diffusing component slightly overshoots its equilibrium value and presents a lower fractional coverage than the one estimated for the single component. The fractional coverage of C3 is not much altered compared to the single-component case, which makes it more selectively adsorbed from the ternary mixture. The fractional occupancy of C2, the species with the highest fractional coverage as single component, is decreased in the mixture, which lowers its selectivity accordingly.

iv. In those cases that $K_2 > K_3$, a cross-over between $S_{2,1}$ and $S_{3,1}$ can occur with pressure

v. The model has proved to be useful for the evaluation of adsorption and diffusion properties in a zeolite-based catalyst.

Although in this study the focus is on zeolite adsorbents, similar transient behavior would be expected for other nanoporous materials. Even if the adsorption and diffusion properties of novel potentially useful nanomaterials (50–53) may be different from those of most common zeolites, similar interaction effects (adsorbate-solid, adsorbate-adsorbate) are expected for the multi-component diffusive transport. Hence, as new studies are carried out for material characterization, the use of models as the one presented herein becomes of paramount importance for the analysis of experimental information.

NOMENCLATURE

A	Adsorbent area ($m^3\ kg^{-1}$)
b	Langmuir adsorption constant (kPa^{-1})
B	Element of the sorbate-sorbate interaction matrix ($s\ m^{-2}$)
B	Sorbate-sorbate interaction matrix ($s\ m^{-2}$)
C1	a fast diffusing-weak adsorbing species
C2	a low diffusing-strong adsorbing species
C3	a high saturation capacity species

D_0	Zero coverage diffusivity ($m^2\ s^{-1}$)
IAST	Isotherm according to the Ideal Adsorbed Solution Theory
K	Henry adsorption constant (mol kg^{-1} kPa^{-1})
m	Mass (kg)
N	Molar flow (mol $s\ m^{-2}$)
$\underline{N}$	Multi-component molar flow vector (mol $s\ m^{-2}$)
P	Pressure (kPa)
q	Local concentration of species adsorbed on the catalyst (mol kg^{-1})
$\bar{q}$	Volume – averaged concentration of species adsorbed on the particle (mol kg^{-1})
$\mathbf{q}_s$	Diagonal matrix of saturation adsorption capacities (mol kg^{-1})
r	Radial length dimension (m)
r_c	Zeolite particle radius (m)
R	Universal gas constant (kPa m^3 mol^{-1} K^{-1})
S	Adsorption selectivity
t	Time (s)
T	Temperature (K)
V	Volume (m^3)
x	mole fraction of the adsorbed phase
y	mole fraction of the gas phase

Greek letters

θ	Fractional coverage
$\bar{\theta}$	Volume-averaged fractional coverage
$\underline{\nabla}\theta$	Multi-component gradient vector of fractional coverage (m^{-1})
$\underline{\nabla} \cdot \underline{N}$	Divergence of the molar flux (mol m^{-3} s^{-1})
π	Spreading pressure (kPa m)
ρ	Density (kg m^{-3})
τ	Adimensional diffusion time
Γ	Thermodynamic correction factor
Γ	Matrix of thermodynamic correction factors

Superscripts

eq	Equilibrium
eq–H	Henry equilibrium
0	Initial condition
*	Indicates reference value in IAST isotherm

Subscripts

gp	Gas phase
i,j	Components *i* or *j*
ij	Cross-term between component *i* and *j*
IAST	IAST isotherm
pure	Pure or single component
s	Adsorption capacity at saturation.
z	zeolite

ACKNOWLEDGMENTS

This work was supported by The National Council for Scientific and Technological Research CONICET.

REFERENCES

1. Sircar, S. (2006) Basic research needs for design of adsorptive gas separation processes. *Ind. Eng. Chem. Res.*, 45: 5435.
2. Wan, Y.S., Hang Chau, J.L., and Gavrilidis, A.K.L. (2001) Design and fabrication of zeolite-based microreactors and membrane microseparators. *Microp. Mesop. Mater.*, 42 (2–3): 157.
3. Kiwi-Minsker, L. and Renken, A. (2005) Microstructured reactors for catalytic reactions. *Catal. Today*, 110 (1–2): 2.
4. Zampieri, A., Colombo, P., Mabande, G.T.P., Selvam, T., Schwieger, W., and Scheffler, F. (2004) Zeolite coatings on microcellular ceramic foams: a novel route to microreactor and microseparator devices. *Adv. Mater.*, 16 (9–10): 819.
5. Vilaseca, M., Coronas, J., Cirera, A., Cornet, A., Morante, J.R., and Santamaria, J. (2003) Use of zeolite films to improve the selectivity of reactive gas sensors. *Catal. Today*, 82: 185.
6. de Jong, J., Lammertink, R.G.H., and Wessling, M. (2006) Membranes and microfluidics: a review. *Lab Chip.*, 6: 1125.
7. Coronas, J. and Santamaria, J. (2004) The use of zeolite films in small-scale and micro-scale applications. *Chem. Eng. Sci.*, 59 (22–23): 4879.
8. Coppens, M.O. and Dammers, A.J. (2006) Effects of heterogeneity on diffusion in nanopores-From inorganic materials to protein crystals and ion channels. *Fluid Phase Equil.*, 241 (1–2): 308.
9. Pampel, A., Engelke, F., Galvosas, P., Krause, C., Stallmach, F., Michel, D., and Ǩärger, J. (2006) Selective multi-component diffusion measurement in zeolites by pulsed field gradient NMR. *Microp. Mesop. Mater.*, 90 (1–3 SPEC. ISS.): 271.
10. Mc Leary, E.E., Jansen, J.C., and Kapteijn, F. (2006) Zeolite based films, membranes and membrane reactors: Progress and prospects. *Microp. Mesop. Mater.*, 90 (1–3 SPEC. ISS.): 198.
11. Fuchs, A.H. and Cheetham, A.K. (2001) Adsorption of guest molecules in zeolitic materials: Computational aspects. *J. Phys. Chem. B.*, 105 (31): 7375.

12. Smit, B. and Krishna, R. (2003) Molecular simulations in zeolitic process design. *Chem. Eng. Sci.*, 58 (3–6): 557.
13. Krishna, R. (2002) Predicting transport diffusivities of binary mixtures in zeolites. *Chem. Phys. Lett.*, 355 (5–6): 483.
14. Krishna, R. and Baur, R. (2003) Modelling issues in zeolite based separation processes. *Separ. Purif. Tech.*, 33: 213.
15. Myers, A.L. and Prausnitz, J.M. (1965) Thermodynamics of mixed-gas adsorption. *AIChE J.*, 11: 121.
16. Kapteijn, F., Moulijn, J.A., and Krishna, R. (2000) The generalized Maxwell-Stefan model for diffusion in zeolites: sorbate molecules with different saturation loadings. *Chem. Eng. Sci.*, 55: 2923.
17. Salem, A., Ghoreyshi, A.A., and Jahanshahi, M. (2006) A multicomponent transport model for dehydration of organic vapors by zeolite membranes. *Desalination.*, 193: 35.
18. Martinek, J.G., Gardner, T.Q., Noble, R.D., and Falconer, J.L. (2006) Modeling transient permeation of binary mixtures through zeolite membranes. *Ind. Eng. Chem. Res.*, 45: 6032.
19. Wirawan, S.K. and Creaser, D. (2006) Multicomponent H2/CO/CO2 adsorption on BaZSM-5 zeolite. *Separ. Purif. Tech.*, 52: 224.
20. Qinglin, H., Farooq, S., and Karimi, I.A. (2003) Binary and ternary adsorption kinetics of gases in carbon molecular sieves. *Langmuir*, 19: 5722.
21. Ruthven, D.M. (1984) *Principles of Adsorption and Adsorption Processes*; John Wiley & Sons: New York.
22. Karger, J. and Ruthven, D.M. (1992) *Diffusion in Zeolites and Other Microporous Solids*; John Wiley & Sons: New York.
23. Krishna, R. and Wesselingh, J.A. (1997) The Maxwell-Stefan approach to mass transfer. *Chemical Engineering Science.*, 52 (6): 861.
24. Vignes, A. (1966) Diffusion in binary solutions. *Industrial and Engineering Chemistry Research.*, 5 (2): 189.
25. Yang, R.T. (1987) *Gas Separation by Adsorption Process*; Butterworth: Boston.
26. Brandani, S., Cavalcante, C., Guimaraes, A., and Ruthven, D.M. (1998) Heat effects in ZLC experiments. *Adsorption.*, 4: 275.
27. Da Silva, F.A. and Rodrigues, A.E. (2001) An analytical solution for the analysis of zero-length-column experiments with heat effects. *Ind. Eng. Chem. Res.*, 40: 3697.
28. van der Linde, S.C., Nijhuis, T.A., Dekker, F.H.M., Kapteijn, F., and Moulijn, J.A. (1997) Mathematical treatment of transient kinetic data: combination of parameter estimation with solving the related partial differential equations. *Applied Catalysis A: General*, 151: 27.
29. Krishna, R. and Baur, R. (2003) Diffusion, adsorption and reaction in zeolites: modelling and numerical issues. http://ct-cr4.chem.uva.nl/zeolite/.
30. Denayer, J.F., Baron, J.B., Souverijns, W., Martens, J.A., and Jacobs, P.A. (1997) *Ind. Eng. Chem. Res.*, 36 (8): 3242.
31. Krishna, R. and Baur, R. (2005) On the Langmuir-Hinshelwood formulation for zeolite catalyzed reactions. *Chem. Eng. Sci.*, 60: 1155.
32. Ruthven, D.M. (2004) Sorption kinetics for diffusion-controlled systems with a strongly concentration-dependent diffusivity. *Chem. Eng. Sci.*, 59: 4531.
33. Lee, C.K., Ashtekar, S., Gladden, L.F., and Barrie, P.J. (2004) Adsorption and desorption kinetics of hydrocarbons in FCC catalysts studied using a tapered element oscillating microbalance (TEOM). Part 1: experimental measurements. *Chem. Eng. Sci.*, 59: 1131.

34. Avila, A.M., Bidabehere, C.M., and Sedran, U. (2007a) Diffusion and adsorption selectivities of hydrocarbons over FCC catalysts. *Chem. Eng. J.*, 132: 67.
35. Stoitsas, K.A., Gotzias, A., Kikkinides, E.S., Steriotis, Th.A., Kanellopoulos, N.K., Stoukides, M., and Zaspalis, V.T. (2005) Porous ceramic membranes for propane-propylene separation via the [pi]-complexation mechanism: unsupported systems. *Microp. Mesop. Mater.*, 78 (2–3): 235.
36. Kouvelos, E., Kesore, K., Steriotis, T., Grigoropoulou, H., Bouloubasi, D., Theophilou, N., Tzintzos, S., and Kanelopoulos, N. High pressure N2/CH4 adsorption measurements in clinoptilolites. *Microp. Mesop. Mater.*, 99 (1–2): 106.
37. Denayer, J.F.M., Daems, I., and Baron, G.V. (2006) Adsorption and reaction in confined spaces. *Oil & Gas Sci. Tech. - Rev. IFP.*, 4 (61): 561.
38. Krishna, R., Calero, S., and Smit, B. (2002) Investigation of entropy effects during sorption of mixtures of alkanes in mfi zeolite. *Chem. Eng. J.*, 88: 81.
39. Calero, S., Smit, B., and Krishna, R. (2001) Configurational entropy effects during sorption of hexane isomers in silicalite. *J. Catal.*, 202: 395.
40. Li, S., Martinek, J.G., Falconer, J.L., Noble, R.D., and Gardner, T.Q. (2005) High pressure CO2/CH4 separation using SAPO-34. *Membranes. Ind. Eng. Chem. Res.*, 44: 3220.
41. Calero, S., Dubbeldam, D., Krishna, R., Smit, B., Vlugt, T.J.H., Denayer, J.F.M., Martens, J.A., and Maesen, L.M. (2004) Understanding the role of sodium during adsorption: a force field for alkanes in sodium-exchanged faujasites. *J. Am. Chem. Soc.*, 126: 11376.
42. Peng, J., Ban, H., Zhang, H., Song, L., and Zhaolin, S. (2005) Binary adsorption equilibrium of propylene and ethylene on silicalite-1: prediction and experiment. *Chem. Phys. Lett.*, 401: 94.
43. Schuring, D., Koriabkina, A.O., de Jong, A.M., Smit, B., and van Santen, R.A. (2001) Adsorption and diffusion of n-Hexane/2-methylpentane mixtures in zeolite silicalite: experiments and modeling. *J. Phys. Chem. B.*, 105: 7690.
44. Cottier, V., Bellat, J.P., and Simonot-Grange, M.H. (1997) Adsorption of p-xylene/m-xylene gas mixtures on BaY and NaY zeolites. Coadsorption equilibria and selectivities. *J. Phys. Chem. B.*, 101: 4798.
45. Buffham, B.A., Mason, G., and Heslop, M.J. (1999) Binary adsorption isotherms from chromatographic retention times. *Ind. Eng. Chem. Res.*, 38: 1114.
46. Yu, M., Hunter, J.T., Falconer, J.L., and Noble, R.D. (2006) *Microp. Mesop. Mater.*, 96: 376.
47. Krishna, R. (2000) Diffusion of binary mixtures in microporous materials: overshoot and roll-up phenomena. *Int. Comm. Heat Mass Transfer.*, 27: 893.
48. de Lasa, H.I. (1992) U.S. Patent 5,102,628.
49. Avila, A.M., Bidabehere, C.M., and Sedran, U. (2007b) Assessment and modelling of adsorption selectivities in the transport of mixtures of hydrocarbons in FCC catalysts. *Ind. Eng. Chem. Res.*, 46: 7927.
50. Sebastian, V., Lin, Z., Rocha, J., Tellez, C., Santamaria, J., and Coronas, J. (2005) A new titanosilicate umbite membrane for the separation of H2. *Chem. Comm.*, 24: 3036.
51. Liu, Q., Wang, T., Liang, C., Zhang, B., Liu, S., Cao, Y., and Qi, J. (2006) Zeolite married to carbon: a new family of membrane materials with excellent gas separation performance. *Chem. Mater.*, 18: 6283.
52. Lines, M.G. (2007) Nanomaterials for practical functional uses. *J. Alloys Comp.*, doi:10.1016/j.jallcom.2006.02.082.
53. Arora, G. and Sandler, S. (2007) Molecular sieving using single wall carbon nanotubes. *Nano Lett.*, 7 (3): 565.